

A Non-Local Stress Failure and Fatigue Damage Accumulation Condition

REFERENCE Seweryn, A. and Mróz, Z., A non-local stress failure and fatigue damage accumulation condition, *Multiaxial Fatigue and Design*, ESIS 21 (Edited by A. Pineau, G. Cailletaud, and T. C. Lindley) 1996, Mechanical Engineering Publications, London, pp. 261–282.

ABSTRACT A non-local stress condition for crack initiation and propagation is proposed and applied to several particular cases. Brittle failure initiation for notched elements under complex loading (Modes I and II) is considered. Values of critical load and crack orientation are predicted from the non-local condition, which is applicable to both regular and singular stress concentrations. Both monotonic and variable loading cases are discussed and conditions for fatigue crack initiation and propagation are proposed. The resulting fatigue crack growth rates are derived starting from the proposed damage evolution rule. The damage evolution for in-phase and out-of-phase bending and torsion is discussed.

1 Introduction

A major problem in fracture mechanics is associated with the formulation of sufficiently simple and accurate conditions of crack initiation and growth in areas of stress concentration. The problem is important in view of the need for reliable predictions of structural elements involving multiaxial stress states. The actual strength predictions are usually based on local stress conditions at non-singular concentrations generated by holes, notches, etc. On the other hand, for existing cracks with singular stress concentrations at their tips, the crack growth is predicted by the process of critical evaluations of the elastic energy release, the strain energy density factor or critical crack opening (1–7). There is no unique condition applicable for both regular and singular stress concentrations. The aim of this paper is to propose such a condition and demonstrate its application to a variety of particular cases, including monotonic and variable loading.

* Faculty of Mechanics, Białystok University of Technology, Wiejska 45C, 15–351 Białystok, Poland.

† Institute of Fundamental Technological Research, Polish Academy of Science, Świerkowska 21, 00–049 Warsaw, Poland.

The condition proposed in this paper is expressed in terms of a non-local measure of stress intensity specified over an assumed finite damage area, representative of the material considered. Multiaxial stress states can be simply analysed for prediction not only of initiation but also of orientation of cracking. For a non-stable crack growth such initiation will inevitably induce a global failure of the element. For variable loading, the fatigue damage accumulation is predicted by specifying proper non-local damage evolution rules and crack initiation conditions. These rules could be applied for predicting fatigue endurance, crack initiation and propagation. In this way, we avoid separate formulations of fatigue crack initiation and propagation criteria, usually proposed in the literature.

In Section 2, the non-local condition will be formulated and applied to the study of crack initiation in notched elements. In Section 3, fatigue damage evolution will be considered and the resulting crack growth criteria will be derived. In Section 4 the cases of in-phase and out-of-phase bending and torsion cyclic loading are considered.

2 Criterion of Initiation and Propagation of Cracks in Plane Structural Elements

We introduce a local polar coordinate system (r, φ) whose origin is placed at the point $\mathbf{x} = (x_0, y_0)$, Fig. 1, referred to a global reference system (x, y) . The point \mathbf{x}_0 is located at the crack tip or in the case of a rounded notch or hole, at the expected crack initiation point.

A proposed stress criterion of brittle failure is based on the assumption that initiation or propagation of cracking occurs when the mean value of the decohesive stress over a specified damaged segment d_0 reaches its critical value (12):

$$R_f = \max_{(\varphi, \mathbf{x}_0)} R(\sigma_n, \tau_n) = \max_{(\varphi, \mathbf{x}_0)} \left[\frac{1}{d_0} \int_0^{d_0} F(\sigma_n, \tau_n) dr \right] = 1 \quad (1)$$

where R_f is the failure factor, $R(\sigma_n, \tau_n)$ is the non-local failure function, σ_n, τ_n are the normal and shear stresses on a physical plane, d_0 is the non-locality or damage zone corresponding to a characteristic size associated with microstructure, for instance grain size, \mathbf{x}_0 is the origin of a local coordinate system (r, φ) , specifying the crack initiation point. The local failure function $F(\sigma_n, \tau_n)$ is an homogeneous function of contact stresses σ_n, τ_n of the first degree. Let us note that equation (1) allows us to determine not only the critical load value but also the location and orientation of the initiated crack. In fact, maximizing equation (1) with respect to \mathbf{x}_0 and φ , both location and orientation are specified. In the case of low stress gradients, the criterion (1) can be replaced by

$$R_f = \max_{(\varphi, \mathbf{x}_0)} R(\sigma_n, \tau_n) \approx F_f = \max_{(\varphi, \mathbf{x}_0)} F(\sigma_n, \tau_n) = 1 \quad (2)$$

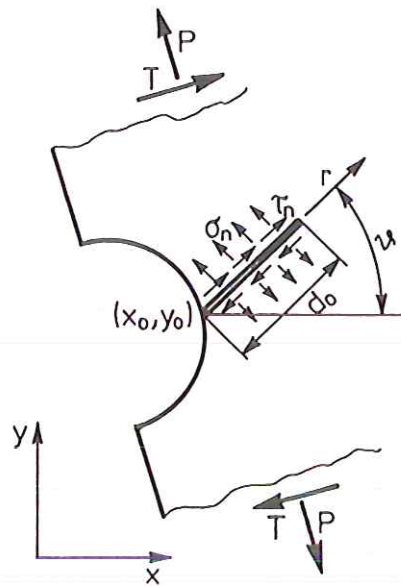


Fig 1 Local polar coordinate system (r, φ) with its origin located at the expected crack initiation point. The stress components σ_n, τ_n induce material decohesion.

where F_f is the local failure factor, and corresponds to the usual local stress conditions of the most intensely stressed elements.

When the maximal tensile condition is used then, analogous to the Novozhilov condition (8), we obtain from equation (1)

$$R_f = \max_{(\varphi, x_0)} R(\sigma_n, \tau_n) = \max_{(\varphi, x_0)} \left[\frac{1}{d_0} \int_0^{d_0} \frac{\sigma_n}{\sigma_c} dr \right] = 1 \quad (3)$$

The condition (3) follows from the assumption that the effect of shear stress on material decohesion is negligible. This assumption, however, is valid for the case of Mode I stress state prevailing near the crack or notch tip. For Modes II and III, the shear stress effect may become significant and cannot be ignored. For a general case for combined loading, the following local failure function is proposed

$$F(\sigma_n, \tau_n) = \left[\left(\frac{\sigma_n}{\sigma_c} \right)^2 + \left(\frac{\tau_n}{\tau_c} \right)^2 \right]^{1/2}, \quad \sigma_n \geq 0 \quad (4a)$$

$$F(\sigma_n, \tau_n) = \frac{|\tau_n|}{\tau_c}, \quad \sigma_n < 0 \quad (4b)$$

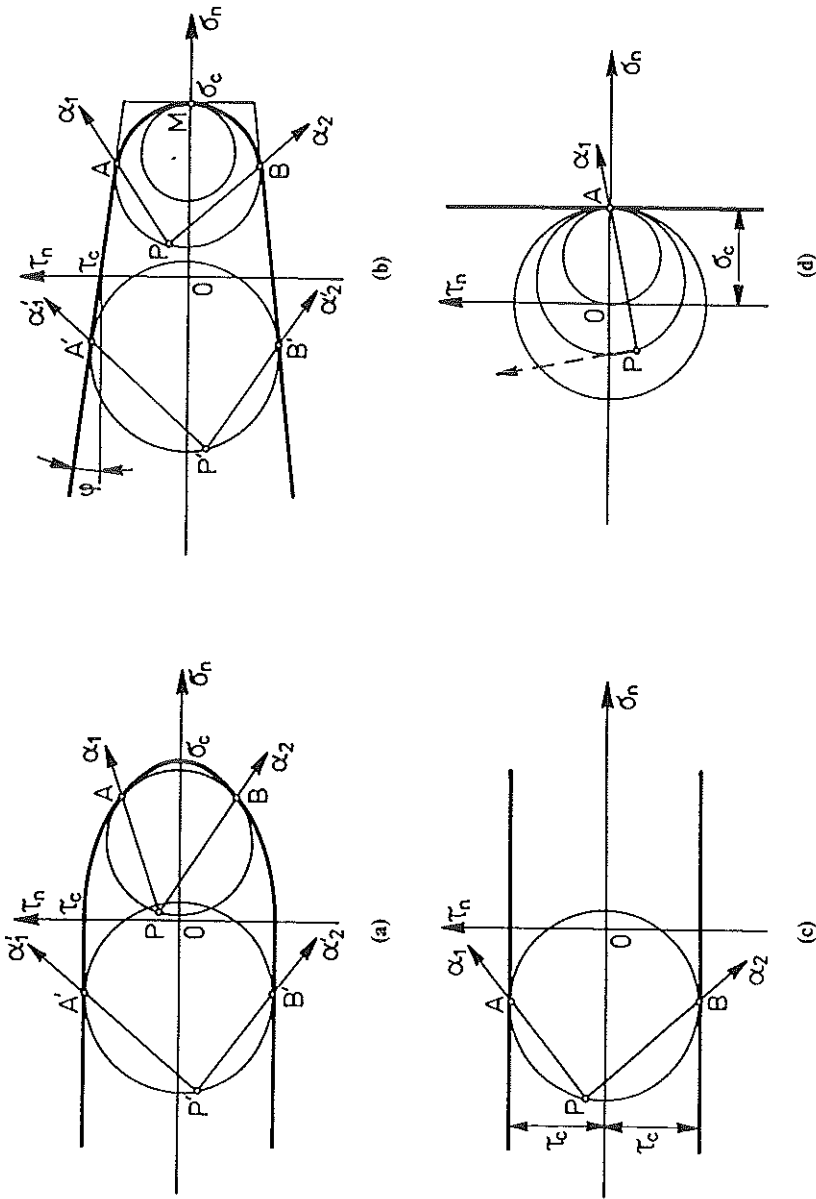


Fig 2 Local failure functions: (a) elliptic condition in tensile regime combined with shear condition in compressive regime; (b) Coulomb condition with tension cut-off; (c) shear condition; (d) tension condition.

where σ_c and τ_c denote the critical rupture stresses of the material in tension and shear. The crack initiation condition is now expressed in terms of nondimensional stresses σ_n/σ_c and τ_n/τ_c

$$R_f = \max_{(\varphi, x_0)} R\left(\frac{\sigma_n}{\sigma_c}, \frac{\tau_n}{\tau_c}\right) = \max_{(\varphi, x_0)} \left[\frac{1}{d_0} \int_0^{d_0} F\left(\frac{\sigma_n}{\sigma_c}, \frac{\tau_n}{\tau_c}\right) dr \right] = 1 \quad (5)$$

The diagram of several failure functions $F(\sigma_n/\sigma_c, \tau_n/\tau_c) - 1 = 0$ is shown in Fig. 2.

In Fig. 2a the elliptic condition equation (4a) and the shear condition equation (4b) are shown in the plane (σ_n, τ_n) . Drawing the stress circles, the extremal planes can be specified as the tangency points of stress circles, the failure function being the envelope to these circles. The planes α_1 and α_2 shown in Fig. 2 are the extreme planes. On the other hand, in the tension régime, only one extreme plane exists as all stress circles are tangential to the failure surface.

Figure 2b presents the Coulomb condition

$$F(\sigma_n, \tau_n) = \frac{1}{\tau_c} (|\tau_n| + \sigma_n \tan \varphi) \quad (6)$$

combined with the tension condition

$$F(\sigma_n, \tau_n) = \sigma_n/\sigma_c \quad (7)$$

The present condition accounts for the effect of friction drag on existing cracks under applied compressive stress, thus requiring larger values of τ_n to produce further crack growth. This condition can be very important in the analysis of cracking of brittle materials deforming in compressive stress regimes. Further, Figs 2c, d present purely shear and tensile conditions. Our analysis in this paper will be solely concerned with the failure condition equation (4), Fig. 2a.

The material parameter d_0 specifies the averaging domain of the failure function (damage zone). This parameter can be identified by requiring the equivalence of the Griffith–Irwin condition and the non-local condition equation (1) in the case of plane cracks in a sheet under remote tension. The stress state in the front of crack tip is then specified by the following relation (3)

$$\sigma_{ij} = \frac{1}{\sqrt{2\pi r}} [K_{I0} a_{ij}(\varphi) + K_{II0} b_{ij}(\varphi)] \quad (8)$$

where r, φ are polar coordinates centred at the tip of a crack, $a_{ij}(\varphi), b_{ij}(\varphi)$ are combinations of trigonometric functions. The stress intensity factors K_{I0} and K_{II0} are defined as follows

$$K_{I0} + iK_{II0} = \lim_{\varphi=0, r \rightarrow 0^+} [\sqrt{2\pi r} (\sigma_{\theta\theta} + i\tau_{r\theta})] \quad (9)$$

For the case of a tensile crack, the Griffith–Irwin condition is

$$K_{I0} = K_{I0c} \quad (10)$$

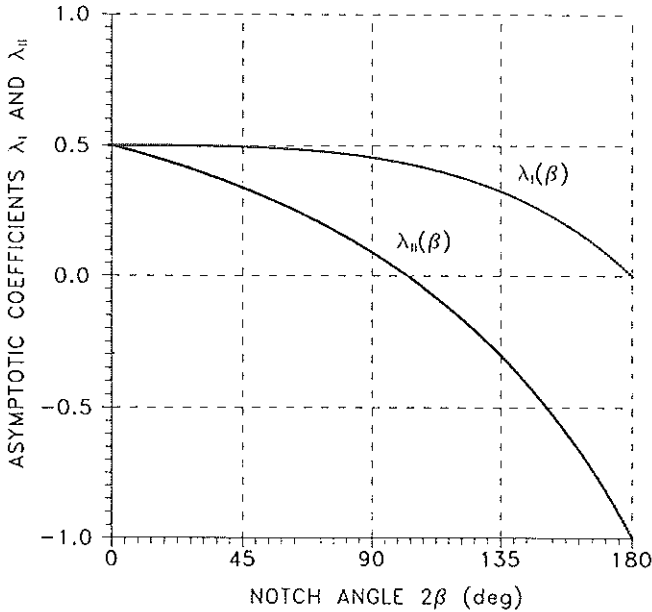


Fig 3 The variation of asymptotic coefficients λ_I and λ_{II} with the notch angle 2β .

Assuming the crack propagation to follow the crack plane, we obtain, by identifying equations (1) and (10) (11)

$$d_0 = \frac{1}{2\pi} \left(\frac{2K_{loc}}{\sigma_c} \right)^2 \quad (11)$$

where the critical stress intensity factor K_{loc} is the material parameter and σ_c , τ_c are the usual rupture stresses determined for homogeneous or nearly homogeneous stress states, such as tension, bending, or torsion ignoring stress gradient effect.

Now some results concerned with the direction of crack propagation and its initiation will be presented for the case of wedge-shaped notches of the angle 2β . The critical values of stress intensity factors K_I and K_{II} inducing crack propagation or initiation will also be determined for a combined mode (Modes I and II) of loading.

The calculations are based on the non-local stress criterion equation (1), using the relation specifying stress distribution near the notch vertex (9, 10)

$$\sigma_{ij} = (2\pi r)^{-\lambda_I} K_I a_{ij}(\varphi) + (2\pi r)^{-\lambda_{II}} K_{II} b_{ij}(\varphi) \quad (12)$$

The general stress intensity factors K_I and K_{II} associated with Mode I and II occurring in equation (12) are defined by the relation

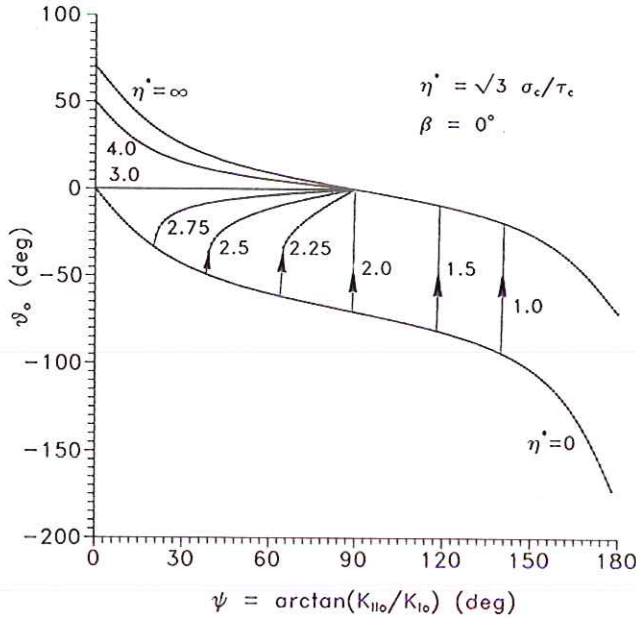


Fig 4 Dependence of crack propagation direction θ_0 on the loading mode K_{II_0}/K_{I_0} for varying ratios σ_c/τ_c .

$$K_I + iK_{II} = \lim_{\varphi \rightarrow 0, r \rightarrow 0+} [(2\pi r)^{\lambda_I} \sigma_\theta + i (2\pi r)^{\lambda_{II}} \tau_{r\theta}] \quad (13)$$

The asymptotic coefficients λ_I and λ_{II} are obtained from the characteristic equations:

$$\sin 2(\lambda_I - 1)\alpha + (\lambda_I - 1) \sin 2\alpha = 0 \quad (14)$$

$$\sin 2(\lambda_{II} - 1)\alpha - (\lambda_{II} - 1) \sin 2\alpha = 0$$

where $\alpha = \pi - \beta$. Figure 3 presents variation of λ_I and λ_{II} with the opening notch angle $0 < \beta < \pi/2$.

A maximum of the non-local failure function $R(\sigma_n, \tau_n)$ with respect to polar coordinate φ has been found using numerical procedure. The cracking was assumed to occur in a plane normal to the plate, initiating from the notch vertex. Figure 4 presents the directions of crack propagation determined from the non-local criterion equation (1) for different values of stress intensity factors K_{I_0} and K_{II_0} and for different values of ratio of rupture stresses σ_c/τ_c . On the abscissa axis, the values of the loading parameter ψ are presented. This parameter is specified by the relation

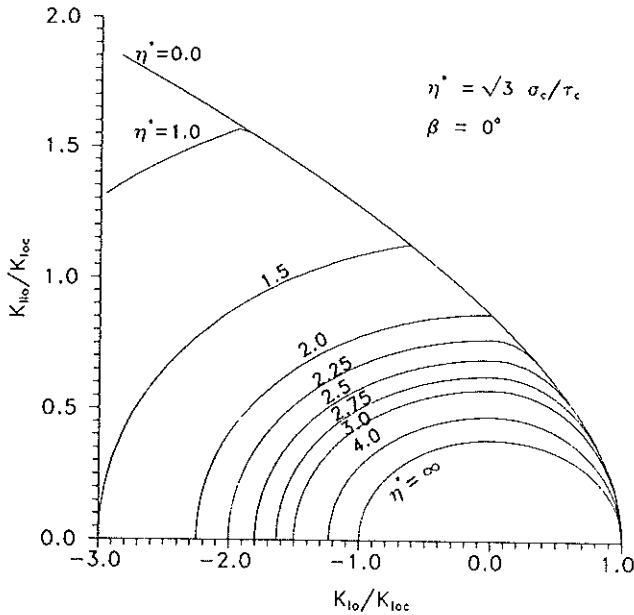


Fig 5 The locus of critical stress intensity factors K_{I0} and K_{II0} in the reference system (K_{I0}/K_{I0c} , K_{II0}/K_{I0c}).

$$K_{II0}/K_{I0} = \tan \psi, K_{II0} \geq 0 \quad (15)$$

The calculated values for the angles φ_0 characterizing the propagation direction are marked by points. The lines with arrows denote discontinuous variation of the direction φ_0 . The values of stress intensity factors K_{I0} and K_{II0} corresponding to the onset of propagation are presented in Fig. 5 for the selected values of σ_c and τ_c . Figure 6 presents the crack propagation directions in vertices of wedge-shaped notches of angles $2\beta = 40^\circ$, for different values of stress intensity factors K_I and K_{II} and for selected ratios σ_c/τ_c . The size of damage zone was assumed as $d_0 = 0.0001$ m, which represent the property of polymethyl methacrylate (Plexiglas). Experiments were carried out for plane plexiglas elements with wedge-shaped notches of angle $2\beta = 40^\circ$ loaded in combined tension and shear. The crack initiation orientation and the critical load were determined for varying ratios of tensile to shear loads. Figure 6 contains the experimental points presenting crack orientation and Fig. 7 presents the evolution of critical values of stress intensity factors K_I and K_{II} . It is seen that there is a good correlation between theoretical predictions following from the non-local condition of equations (1) and (4) and experimental data.

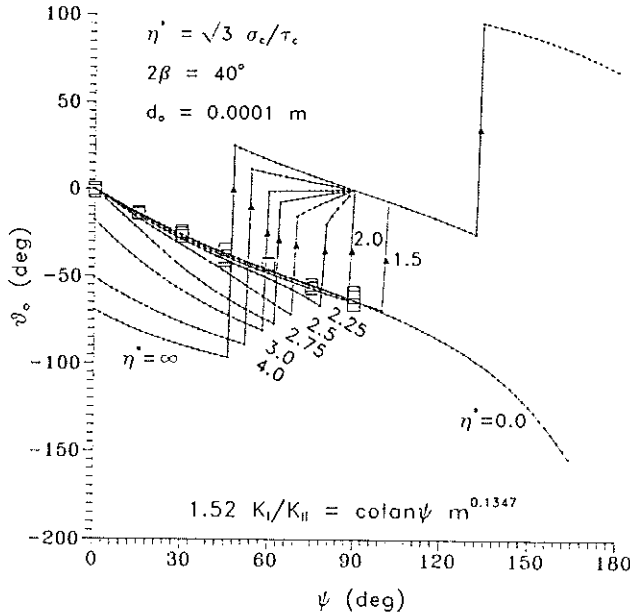


Fig 6 Directions of crack propagation at the vertex of wedge-shaped notch of angle $2\beta = 40^\circ$ in function of (K_I/K_{II}) for different values of σ_c and τ_c (\square - experimental data for plexiglas).

3 Crack Initiation and Propagation Condition For Multiaxial Fatigue Loading

In this section, we shall consider the case of variable multiaxial loading inducing fatigue initiation and growth of cracks. There are numerous criteria for multiaxial fatigue proposed in the literature (13-16). The assessment of fatigue crack growth criteria was recently presented by Ramulu and Kobayashi (26) who also provided comparison with experimental data. The importance of higher-order terms in asymptotic expansion (T-stress effect) was emphasized. In the present work, the local failure function $F(\sigma_n/\sigma_c, \tau_n/\tau_c)$ discussed in Section 2 will now be used together with the non-local condition equation (1) in order to assess fatigue damage accumulation and crack initiation or propagation. The advantage of this approach lies in the fact that the crack growth stage does not require separate formulation but is described by the same type of damage evolution rule to within the material constants. The non-local T-stress effect is naturally incorporated in our formulation.

In the local coordinate system (r, φ) with its origin at the point $x_0(x_0, y_0)$. Fig. 1, the non-local damage condition can be written as

$$R_{of} = \max_{(\varphi, x_0)} R_0 \left(\frac{\sigma_n}{\sigma_0}, \frac{\tau_n}{\tau_0} \right) = \max_{(\varphi, x_0)} \left[\frac{1}{d_0} \int_0^{d_0} F_0 \left(\frac{\sigma_n}{\sigma_0}, \frac{\tau_n}{\tau_0} \right) dr \right] = 1 \quad (16)$$

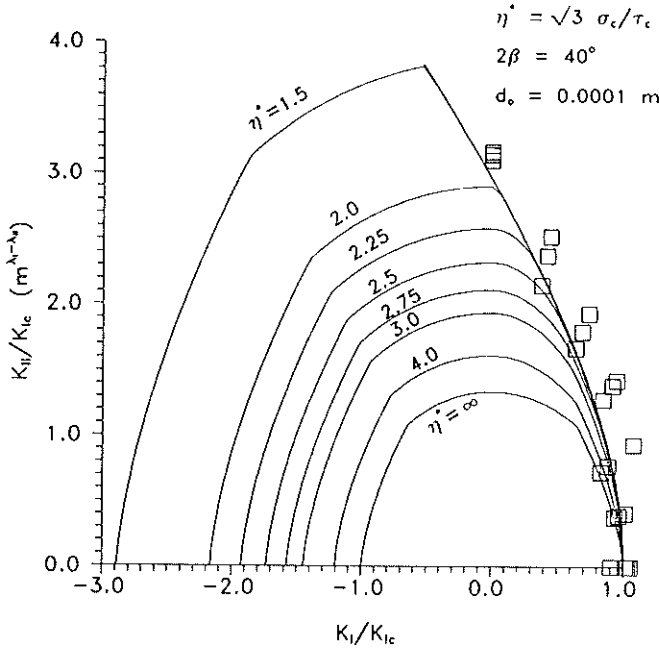


Fig 7 Critical values of generalized stress intensity factors K_I and K_{II} for wedge-shaped notch of angle $2\beta = 40^\circ$ in the reference system (K_I/K_{Ic} , K_{II}/K_{Ic}) (\square - experimental data for Plexiglas).

where R_{of} is the damage initiation factor. The damage accumulation occurs when the averaged value of the local damage initiation function $F_0(\sigma_n/\sigma_0, \tau_n/\tau_0)$ over the damage zone d_0 exceeds the critical value. Here $R_0(\sigma_n/\sigma_0, \tau_n/\tau_0)$ is the non-local damage initiation function measured with respect to its threshold value $R_{of} = 1$ corresponding to the onset of the fatigue process. The parameters σ_0, τ_0 specify the permanent fatigue strength of the material.

When small stress gradients occur, the non-local condition equation (16) can be replaced by the local condition, namely

$$R_{of} = \max_{(\varphi, x_0)} R_0 \left(\frac{\sigma_n}{\sigma_0}, \frac{\tau_n}{\tau_0} \right) \approx \max_{(\varphi, x_0)} F_0 \left(\frac{\sigma_n}{\sigma_0}, \frac{\tau_n}{\tau_0} \right) = 1 \quad (17)$$

A form of the local damage initiation function $F_0(\sigma_n/\sigma_0, \tau_n/\tau_0)$ can be similar to that of the monotonic local failure function $F(\sigma_n/\sigma_c, \tau_n/\tau_c)$, specified by equations (4, 6 or 7). The failure stress parameters σ_c, τ_c are now replaced by fatigue stress parameters $\sigma_0 \leq \sigma_c, \tau_0 \leq \tau_c$ (cf. Fig. 8).

Consider a domain Ω in the plane (σ_n, τ_n) bounded by the curve $F_0 = 1$ representing permanent fatigue strength and the local failure function $F_f = 1$. When the local condition applies, the fatigue damage accumulation occurs for

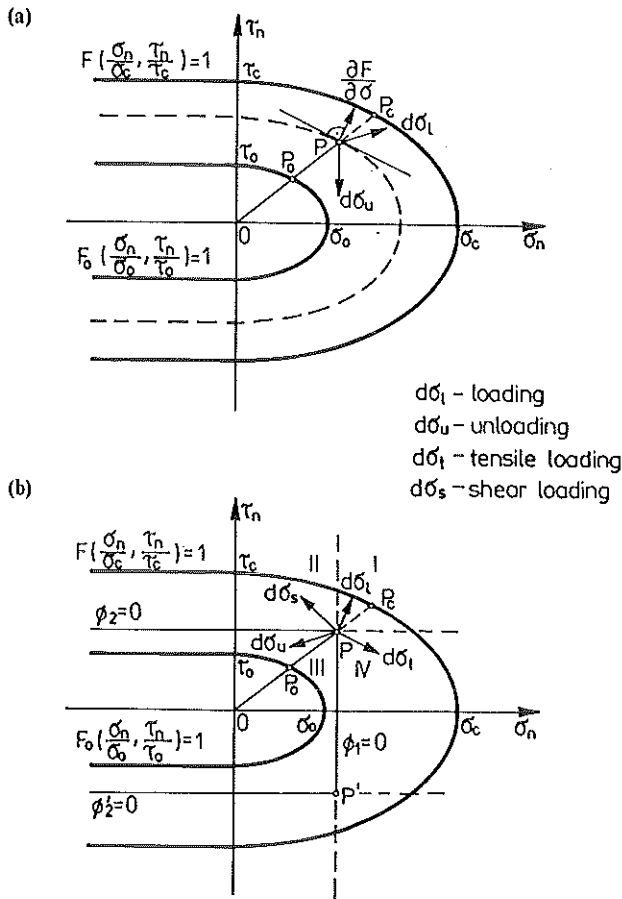


Fig 8 Local failure and damage initiation curves: (a) loading/unloading conditions associated with the function $F - C \leq 0$; (b) loading/unloading conditions associated with the functions $\phi_1 \leq 0$ and $\phi_2 \leq 0$.

stress paths lying in the domain Ω . Assume first, for simplicity, that $\sigma_0/\sigma_c = \tau_0/\tau_c = f$ so the curves $F_0 = 1$ and $F_f = 1$ are similar, Fig. 8a. Introduce within Ω the one-parameter family of curves $F = \text{const.}$ specified by equation (4); then $F = f$ for stress states on the fatigue strength curve $F_0 = 1$, $F = F_f = 1$ for the failure states, and $f \leq F \leq 1$ within the domain Ω . The local crack initiation condition for multiaxial loading and small stress gradients is assumed to be in the form

$$F_d = \max_{(\varphi, x_0)} \left[\int_0^{f_d} A_1 \left(\frac{F-f}{1-f} \right)^n \frac{d\hat{F}}{1-f} \right] = 1 \tag{18}$$

where the parameters A_1 and n specify the damage evolution rate, and

$$d\hat{F} = \begin{cases} dF & \text{for } dF > 0 \text{ and } F - f > 0 \\ 0 & \text{for } dF < 0 \text{ or } F - f \leq 0 \end{cases} \quad (19)$$

$$dF = \frac{\partial F}{\partial \sigma_n} d\sigma_n + \frac{\partial F}{\partial \tau_n} d\tau_n = \begin{cases} \frac{1}{F} \left(\frac{\sigma_n d\sigma_n}{\sigma_c^2} + \frac{\tau_n d\tau_n}{\tau_c^2} \right) & \text{for } \sigma_n \geq 0 \\ \frac{1}{\tau_c} |d\tau_n| & \text{for } \sigma_n < 0 \end{cases} \quad (20)$$

The damage accumulation rule equation (18) specifies the scalar damage measure F_d whose critical value, $F_d = 1$, corresponds to the initiation of a macrocrack on the critical plane. The damage is assumed to accumulate only for stress path portions directed in the exterior of the domain bounded by the curve $F = \text{const.}$ corresponding to the stress point P , and to depend on the distance of P from the fatigue onset curve $F_0 = 1$. In fact, referring to Fig. 8a, we have

$$\left(\frac{F - f}{1 - f} \right)^n = \left(\frac{P - P_0}{P_c - P_0} \right)^n \quad (21)$$

For the non-local condition, assume the R -function to exceed the threshold value \bar{R} corresponding to $R_{\text{of}} = 1$ and to be less than the monotonic failure value $R = R_f = 1$, so that $\bar{R} \leq R \leq 1$. The crack initiation for multiaxial loading is assumed to be generated by the condition analogous to equation (18), namely

$$R_d = \max_{(\varphi, x_0)} \left[\int_0^{\hat{R}_d} A_1 \left(\frac{R - \bar{R}}{1 - \bar{R}} \right)^n \frac{d\hat{R}}{1 - \bar{R}} \right] = 1 \quad (22)$$

where R_d is the non-local damage accumulation measure. The existing crack growth is specified by a similar equation

$$da = \max_{(\varphi, x_0)} \left[A_2 \left(\frac{R - \bar{R}}{1 - \bar{R}} \right)^n \frac{d\hat{R}}{1 - \bar{R}} \right] \quad (23)$$

where A_2 is the crack growth material parameter. The growth factor $d\hat{R}$ is specified according to equations (19) and (20), namely

$$d\hat{R} = \frac{1}{d_0} \int_0^{d_0} d\hat{F} \, dr \quad (24)$$

When similarity of the curves $F_0 = 1$ and $F_f = 1$ is not preserved, that is $\sigma_0/\sigma_c \neq \tau_0/\tau_c$, the damage evolution rules in equations (18) and (22) remain valid. However, along the fatigue onset curve $F_0 = 1$ the value of f is not constant but depends on the stress state; thus $f = f(\sigma_n, \tau_n)$.

The loading/unloading conditions specified by equations (19) and (20) are associated with the curves $F = \text{const.}$ An alternative way of generating these conditions could be proposed by introducing the unloading and loading domains in the stress plane (σ_n, τ_n) specified by the inequalities, Fig. 8b

$$\phi_1 = \hat{\sigma}_n - \sigma_n^+(t) \leq 0 \quad (25)$$

$$\phi_2 = \tau_n^2 - \hat{\tau}_n^2(t) \leq 0$$

where $\sigma_n^+(t)$, $\tau_n(t)$ are the actual values of the tensile normal stress, $\sigma_n^+(t) > 0$, and the shear stress, while $\hat{\sigma}_n$ and $\hat{\tau}_n$ are the subsequent stress states. The conditions of equation (25) specify four loading and unloading angular domains I, II, III, IV at the stress point P, moving with P in the stress plane. The damage accumulation thus occurs when

$$\phi_1 = 0, d\phi_1 > 0, \quad \text{or} \quad \hat{\sigma}_n = \sigma_n^+(t), d\sigma_n > 0 \quad (26)$$

$$\phi_2 = 0, d\phi_2 > 0, \quad \text{or} \quad \hat{\tau}_n^2 = \tau_n^2(t), \tau_n d\tau_n > 0$$

We have therefore

$$d\hat{F} = \frac{\partial F}{\partial \sigma_n} d\hat{\sigma}_n + \frac{\partial F}{\partial \tau_n} d\hat{\tau}_n \quad (27)$$

where

$$d\hat{\sigma}_n = \begin{cases} d\sigma_n & \text{for } d\sigma_n \geq 0 \text{ and } \sigma_n \geq 0 \\ 0 & \text{for } d\sigma_n < 0 \text{ or } \sigma_n < 0 \end{cases} \quad (28)$$

$$d\hat{\tau}_n = \begin{cases} d\tau_n & \text{for } \tau_n d\tau_n \geq 0 \\ 0 & \text{for } \tau_n d\tau_n < 0 \end{cases}$$

Obviously, more complex loading/unloading conditions could be formulated by introducing unloading domains dependent on the prior prestress; similarly to multisurface hardening description, (17).

A general form of crack initiation condition can be stated as follows

$$R_d = \max_{(\varphi, x_0)} \left[\int_0^{\hat{R}_d} A_1 \Psi(R) d\hat{R} \right] = 1 \quad (29)$$

where R_d is the damage accumulation measure and $\Psi(R)$ is the damage accumulation function. The crack propagation condition is formulated similarly

$$da = \max_{(\varphi, x_0)} [A_2 \Psi(R) d\hat{R}] \quad (30)$$

These conditions can obviously be restated in more familiar forms in terms of maximal and minimal stresses or stress intensity factors. Consider, for instance, the case of tensile cyclic loading with minimal stress $\sigma_{\min} = 0$. The crack initiation condition equation (18), now provides the critical number of cycles

$$\log N = -(n+1) \log \left(\frac{\sigma_{\max} - \sigma_0}{\sigma_c - \sigma_0} \right) \text{ for } \sigma_{\min} = 0 \quad (31)$$

where σ_0 is the fatigue strength limit and σ_c is failure stress.

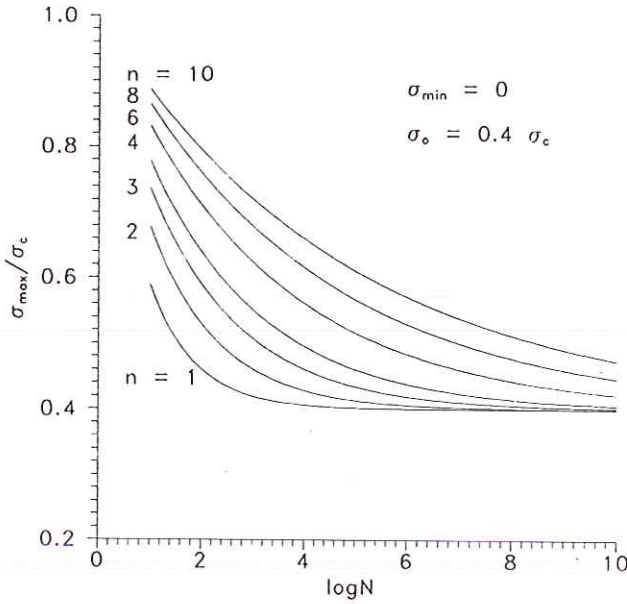


Fig 9 Maximal stress dependence on number of cycles for varying values of the exponent n resulting from equation (31).

Figure 9 presents the maximal stress dependence on the number of cycles for varying values of the exponent n resulting from the condition of equation (31).

The crack propagation condition in Mode I due to cyclic loading can be generated from equation (22) in the form

$$\frac{da}{dN} = C \left[\left(\frac{\langle K_{max} - K_{th} \rangle}{K_c - K_{th}} \right)^{n+1} - \left(\frac{\langle K_{min} - K_{th} \rangle}{K_c - K_{th}} \right)^{n+1} \right] \quad (32)$$

where K_{max} and K_{min} are the maximal and minimal values of the stress intensity factor in particular loading cycle, K_{th} is the threshold value of K corresponding to onset of fatigue, K_c is the critical value of the stress intensity factor, C and n are the material parameters. The bracket symbol $\langle \rangle$ denotes: $\langle g \rangle = g$ for $g > 0$ and $\langle g \rangle = 0$ for $g < 0$. It is seen that equation (32) is similar to familiar rules of fatigue crack propagation due to Paris (20)

$$\frac{da}{dN} = C(K_{max} - K_{min})^m = C(\Delta K)^m \quad (33)$$

or due to Donahue *et al.* (21), Klesnil and Lukas (22), or Cooke and Beevers (23), namely

$$\frac{da}{dN} = C_o(K_a^m - K_{th}^m) \quad (34)$$

where $K_a = (K_{max} - K_{min})/2$.

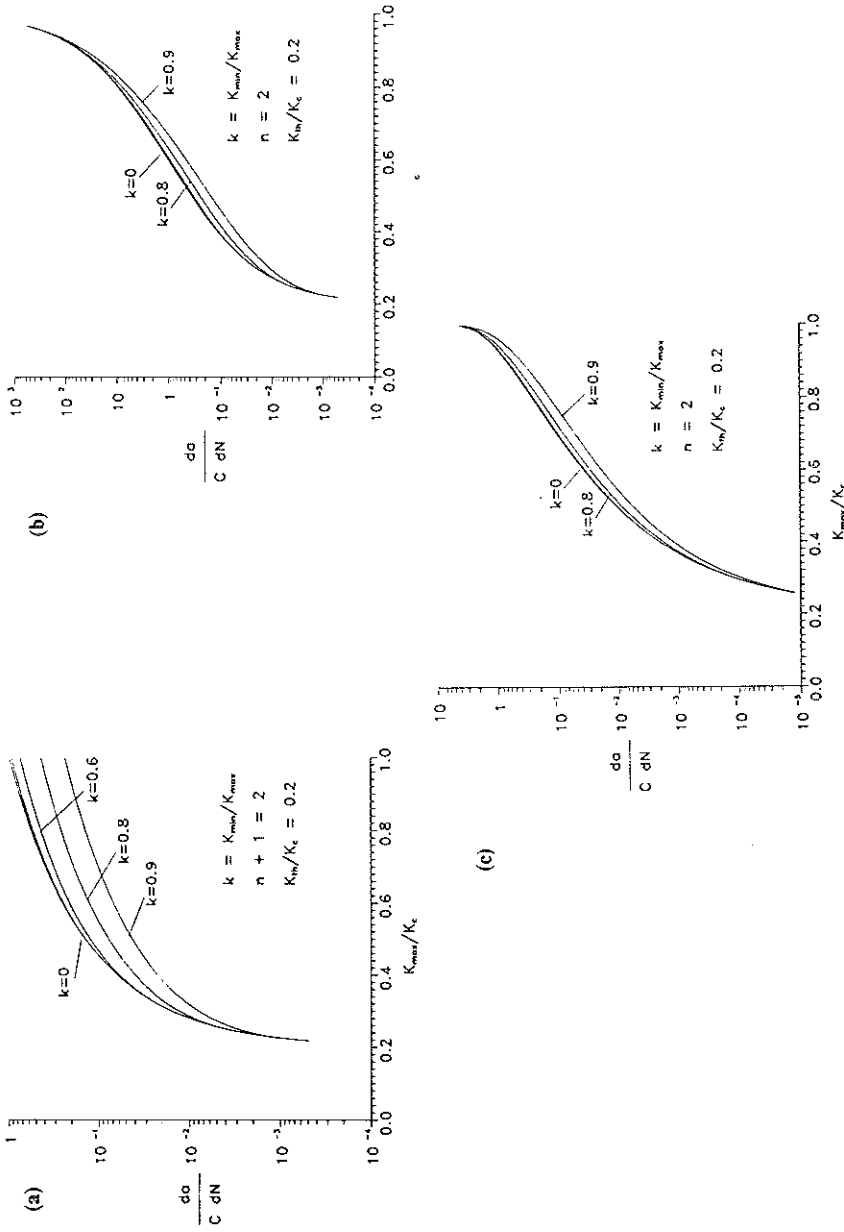


Fig 10 Dependence of fatigue crack growth da/dN on the maximal value of stress intensity factor K_{max} specified from the criteria: (a) equation (32); (b) equation (36); (c) equation (40).

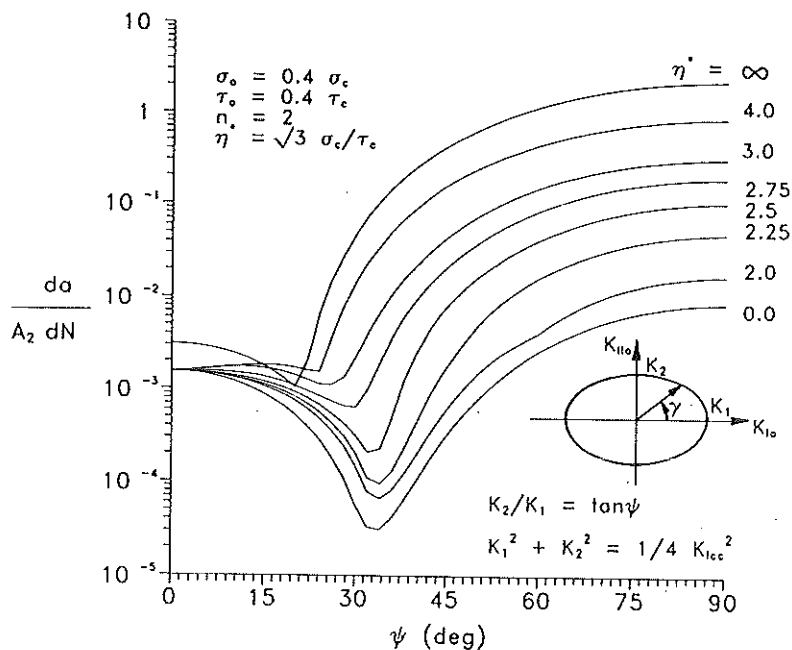


Fig 11 Dependence of crack growth per cycle da/dN on the loading ratio K_1/K_2 for different values of σ_c/τ_c .

Assume now that the damage accumulation function has the following form

$$\Psi(R) = \frac{(R - \bar{R})^{n-1}}{(1 - R)^{n+1}} (1 - \bar{R}) \quad (35)$$

The corresponding fatigue crack propagation condition for tensile cyclic loading is expressed as follows

$$\frac{da}{dN} = C \left[\left(\frac{\langle K_{\max} - K_{th} \rangle}{K_c - K_{\max}} \right)^n - \left(\frac{\langle K_{\min} - K_{th} \rangle}{K_c - K_{\min}} \right)^n \right] \quad (36)$$

This condition is similar to that proposed by Priddle (24), namely

$$\frac{da}{dN} = C \left(\frac{\Delta K - K_{th}}{K_c - K_{\max}} \right)^2 + C' \quad (37)$$

and by Yarema (25)

$$\frac{da}{dN} = C_0 \left(\frac{K_{\max} - K_{th}}{K_c - K_{\max}} \right)^q \quad (38)$$

where C , C' , C_0 and q are material parameters.

A more complex form of the damage accumulation function

$$\Psi(R) = \frac{(R - \bar{R})^n}{(1 - \bar{R})^{n+1}} - \frac{(R - \bar{R})^n}{(1 - \bar{R})^{n+1} - (R - \bar{R})^{n+1}} \quad (39)$$

provides the following crack propagation condition

$$\frac{da}{dN} = -C \left[\frac{\langle K_{\max} - K_{th} \rangle^n - \langle K_{\min} - K_{th} \rangle^n}{(K_c - K_{th})^n} + \ln \frac{(K_c - K_{th})^n - \langle K_{\max} - K_{th} \rangle^n}{(K_c - K_{th})^n - \langle K_{\min} - K_{th} \rangle^n} \right] \quad (40)$$

This condition is similar to that derived by Cherepanov (7) who used the concept of constant dissipation rate per unit crack area growth, namely

$$\frac{da}{dN} = -C \left[\frac{K_{\max}^2 - \langle K_{\min} \rangle^2}{K_c^2} + \ln \frac{K_c^2 - K_{\max}^2}{K_c^2 - \langle K_{\min} \rangle^2} \right] \quad (41)$$

The predicted rates of crack growth from the conditions of equations (32, 36, 40) are plotted in Figs 10a, b, c. It is seen that proper formulation of the non-local crack propagation condition is essential in providing quantitative description of fatigue crack growth.

This fracture initiation and propagation criterion makes it possible to analyse any type of variable loading. For different values of the normal to shear stress ratios the calculations of crack growth per cycle of loading were carried out. The stress intensity factor values vary according to the following relationships

$$K_{I0} = K_1 \cos \gamma, \quad K_{II0} = K_2 \sin \gamma, \quad \gamma = \gamma(t) \quad (42)$$

and they can be represented in the (K_{I0}, K_{II0}) plane as an ellipse with semiaxes equal to K_1 and K_2 . An increment of crack length per cycle versus the loading ratio $K_2/K_1 = \tan \psi$ is shown in Fig. 11 for different values of material failure stresses σ_c and τ_c . The following values are taken in the present case as in example: $\sigma_0 = 0.4\sigma_c$, $\tau_0 = 0.4\tau_c$, $n = 2$ and $K_1^2 + K_2^2 = 0.25K_{loc}^2$. It should be noted that in this mode of loading the crack growth rate is greater for in-plane shear than for simple tension.

4 Fatigue Strength of Elements Subjected to Combined Bending and Torsion

4.1 In-phase loading problem

Consider now a cylindrical specimen subjected to combined cyclic loading by bending and torsional moments. These moments acting in-phase induce axial and shear stresses of amplitudes σ_a and τ_a and mean values $\sigma_m = \tau_m = 0$. Assume the circumferential stresses to vanish, $\sigma_\theta = 0$. Using the Mohr's circle, Fig. 12, the stresses can be represented as follows

$$\sigma_n = \sigma_{no} + k \cos 2\varphi; \quad \tau_n = k \sin 2\varphi \quad (43)$$

where

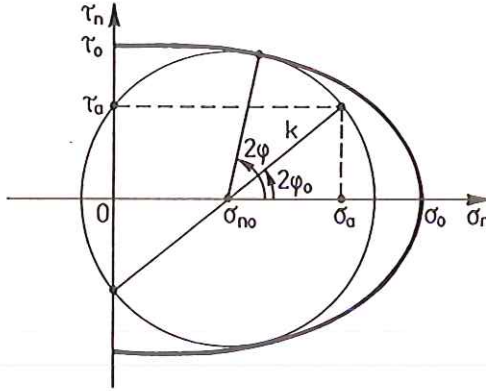


Fig 12 Mohr circle representing stress state in an element under bending and torsion.

$$\sigma_{no} = \frac{\sigma_a}{2}, \quad k^2 = \left(\frac{\sigma_a}{2}\right)^2 + \tau_a^2$$

The local damage initiation condition equation (17) (for the case of small stress gradients) now has the form

$$R_{of} = \max_{(\varphi)} R_0 = \max_{(\varphi)} \left[\left(\frac{\sigma_n}{\sigma_0}\right)^2 + \left(\frac{\tau_n}{\tau_0}\right)^2 \right]^{1/2} = 1 \tag{44}$$

Using equation (43), we have

$$R_{of} = \max_{(\varphi)} \left[\frac{\left(\sqrt{\frac{\sigma_a^2}{4} + \tau_a^2} \cos 2\phi + \frac{\sigma_a}{2} \right)^2}{\sigma_0^2} + \frac{\left(\frac{\sigma_a^2}{4} + \tau_a^2 \right) \sin^2 2\phi}{\tau_0^2} \right]^{1/2} = 1 \tag{45}$$

The condition of maximum of R_0 , $\partial R_0 / \partial \phi = 0$, provides

$$\sin 2\phi = 0 \tag{46a}$$

or

$$\cos 2\phi = \frac{\sigma_a}{2(\eta^2 - 1)k} \tag{46b}$$

where $\eta = \sigma_0 / \tau_0$.

The condition of equation (46a) is equivalent to the condition of maximal normal stress, since for equation (46a) there is $\tau_{ac} = \sigma_{ac} = \sigma_0$, Fig. 12. Here τ_{ac} and σ_{ac} are the limit values of stress amplitudes σ_a and τ_a for the case of separate action of torsion and bending moments. The local condition equation (45) can now be expressed as follows

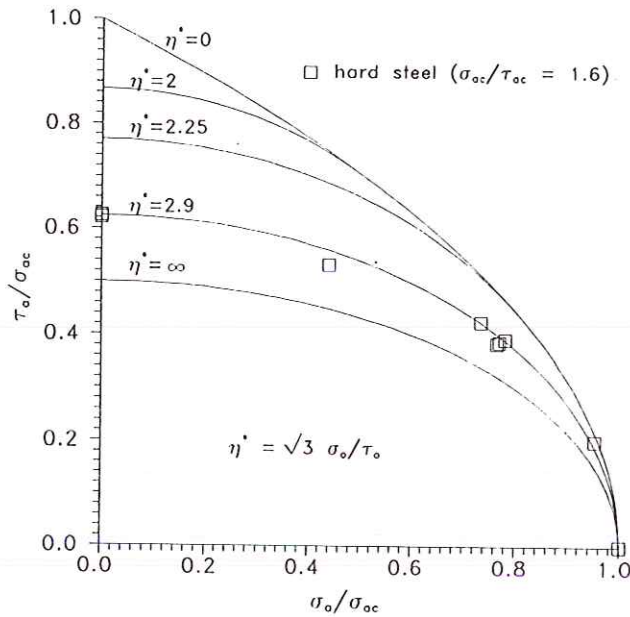


Fig 13 Fatigue onset curves in the plane $(\sigma_a/\sigma_{ac}, \tau_a/\tau_{ac})$ for different values of $\eta^* = \sqrt{3}\sigma_0/\tau_0$ (\square - experimental data for hard steel).

$$\psi_1 = \frac{\tau_a^2}{\tau_{ac}^2} + \frac{\sigma_a}{\sigma_{ac}} = 1 \quad (47)$$

Let us note that equation (47) is similar to the condition proposed by Gough *et al.* (19).

The condition of equation (46b) leads to the elliptical condition of Gough and Pollard (18)

$$\psi_2 = \frac{\sigma_a^2}{\sigma_{ac}^2} + \frac{\tau_a^2}{\tau_{ac}^2} = 1 \quad (48)$$

where

$$\sigma_{ac}^2 = \sigma_0^2 \frac{4(\eta^2 - 1)}{\eta^4}; \quad \tau_{ac} = \tau_0$$

In a general case of combined bending and torsion, the fatigue onset condition can be expressed as follows

$$\max(\psi_1, \psi_2) = 1 \quad (49)$$

When $\eta < 1$, the maximal normal stress condition equation (47) applies; when $\eta > \sqrt{2}$, the elliptical condition (48) is valid. For intermediate values of η ,

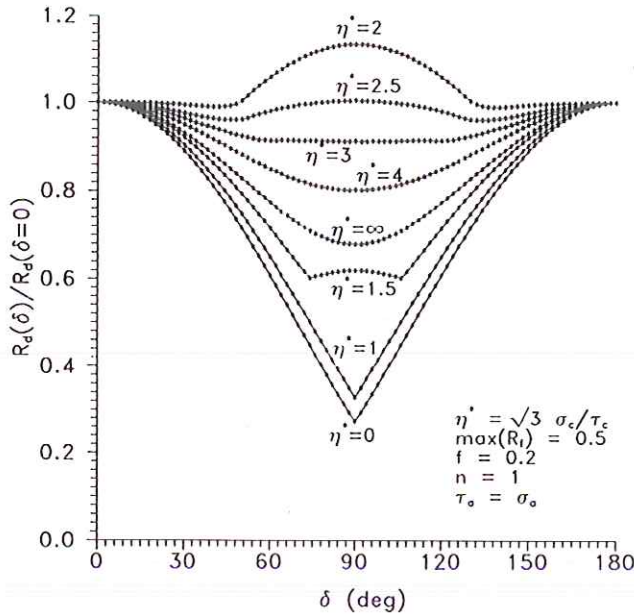


Fig 14 Dependence of damage accumulation factor R_d on the loading phase shift angle δ .

($1 < \eta < \sqrt{2}$), the form of condition depends on the stress amplitude σ_a . In fact, when

$$\frac{\sigma_a}{2\sigma_o} \geq 1 - \left(\frac{\tau_o}{\sigma_o}\right)^2 = \frac{\eta^2 - 1}{\eta^2} \quad (50)$$

then the condition (47) applies, but when equation (50) is not satisfied, the condition (48) is valid. Figure 13 presents the fatigue onset curves in the plane (σ_a/σ_{ac} , τ_a/τ_{ac}) for different values of η . The experimental data for hard steel ($\sigma_{ac}/\tau_{ac} = 1.6$) provide good correlation with our prediction for $\sqrt{3}\eta = 2.9$.

The predicted crack orientation φ_r measured with respect to plane normal to specimen axis is expressed by the formula

$$\varphi_r = \pm \varphi - \varphi_o, \quad \varphi_o = \frac{1}{2} \arctan \frac{2\tau_a}{\sigma_a} \quad (51)$$

where φ is specified from the condition of equations (46a) or (46b). As for equation (46a) where $\varphi = 0$, there is only one critical plane. On the other hand, the condition of equation (46b) implies existence of two critical planes of crack initiation.

4.2 The case of out-of-phase loading

Consider now a cylindrical specimen subjected to bending and torsion and the stress loading program

$$\sigma(t) = \sigma_a \sin(\omega t), \quad \tau(t) = \tau_a \sin(\omega t - \delta) \quad (52)$$

where σ_a and τ_a are respectively the amplitudes of the normal stress due to bending and of the shear stress due to torsion, δ is the phase shift angle.

Let us use in this case the local crack initiation condition of equation (18) with $\sigma_0 = f\sigma_c$, $\tau_0 = f\tau_c$, $0 \leq f \leq 1$. Then we have $F(\sigma_n, \tau_n) = fF_0(\sigma_n, \tau_n)$ and the damage accumulation measure R_d is given by equations (18) and (27).

Figure 14 presents the dependence of damage accumulation factor R_d on the phase shift angle δ . The value of stress amplitude was assumed for which the damage factor F_f for $\delta = 0$ reached maximum. It is seen that the phase shift angle δ may increase or decrease the fatigue strength depending on the value of σ_c/τ_c .

5 Concluding Remarks

The non-local brittle failure criterion discussed in this paper provides the critical stress value for crack initiation and also for existing crack propagation in structural elements under complex loading conditions. It can also be used to determine the crack initiation or propagation direction. Both regular and singular stress concentrations can be treated in a uniform way, with transition to local stress criteria for small stress gradients or to energy criteria for singular stress distributions. The main material parameters are σ_c , τ_c and d_0 . The size d_0 of the damage zone is specified by a material microstructure, for instance grain size. The failure function $F(\sigma_n, \tau_n)$ provides the assessment of failure on specific physical planes with its maximal value reached on one or two planes. Tensile shear or combined failure modes may occur depending on values of σ_c , τ_c and d_0 .

The present approach may therefore prove useful in engineering calculations of onset and propagation of cracking in structural elements undergoing brittle fracture. Its extension to the case of cyclic loading and fatigue problems discussed in this paper provides new fatigue conditions which require further study. It should be emphasized that both fatigue crack initiation and propagation rules are generated by the same type of non-local condition.

When plastic deformation predominates, the approach should be modified to account for stress redistribution due to the plastic strain field. The failure mode is then mainly governed by strain localization effects and generation of shear bands which become consecutively the failure zones. The low-cycle fatigue conditions should be formulated taking account of transient or steady elasto-plastic stress distributions.

References

- (1) ERDOGAN, F. and SIH, G. C. (1963) On the crack extension of plates under plane loading and transverse shear, *J. Basic Engineering*, **85**, pp. 519–527.
- (2) GRIFFITH, A. A. (1920) The phenomena of rupture and flowing solids, *Phil. Trans. R. Soc. A.*, **221**, pp. 163–198.
- (3) IRWIN, G. (1957) Analysis of stresses and strains near the end of crack traversing a plate, *J. Appl. Mech.*, **24**, pp. 361–365.
- (4) RICE, J. R. (1968) A path-independent integral and the approximate analysis of strain concentration by notches and cracks, *J. Appl. Mech.*, **15**, pp. 379–386.
- (5) SIH, G. C. (1974) Strain-energy-density factor applied to mixed mode crack problems, *Int. J. Fracture*, **10**, pp. 305–321.
- (6) WELLS, A. A. (1961) Critical tip opening displacement as fracture criterion, in: *Proc. Crack Propagation Symp.*, Cranfield, **1**, 210–221.
- (7) CHEREPANOV, G. P. (1979) *Mechanics of Brittle Fracture*, McGraw-Hill, New York.
- (8) NOVOZHILOV, V. V. (1969) On necessary and sufficient criterion of brittle fracture, (in Russian), *Prikl. Mat. Mech. (PMM)*, **33**, pp. 212–216.
- (9) WILLIAMS, M. L. (1952) Stress singularities resulting from various boundary conditions in angular corners of plates in extension, *J. Appl. Mech.*, **19**, pp. 526–528.
- (10) SEWERYN, A. and ZWOLINSKI, J. (1993) Solution for the stress and displacement fields in the vicinity of a V-notch of negative wedge angle in plane problems of elasticity, *Engng Fract. Mech.*, **44**, pp. 275–281.
- (11) SEWERYN, A. (1994) Brittle fracture criterion for structures with sharp notches, *Engng Fract. Mech.*, **47**, 673–681.
- (12) SEWERYN, A. and MROZ, Z. (1995) A non-local stress failure condition for structural elements under multiaxial loading, *Engng Fract. Mech.*
- (13) STULEN, F. B. and CUMMINGS, H. N. (1954) A failure criterion for multiaxial fatigue stresses, *Proc. ASTM*, **54**, pp. 822–835.
- (14) MATAKE, T. (1977) An explanation on fatigue limit under combined stress, *Bull. JSME*, **20**, pp. 257–263.
- (15) McDIARMID, D. L. (1991) A general criterion for high-cycle multiaxial fatigue failure, *Fatigue Fract. Eng. Mat. Struct.*, **14**, pp. 429–453.
- (16) PAPADOPOULOS, I. V. and DANG VAN, K. (1988) Sur la nucleation des fissures en fatigue polycyclique sous chargement multiaxial, *Arch. Appl. Mech.*, **40**, pp. 759–774.
- (17) MROZ, Z. (1983) Hardening and degradation rules for metals under monotonic and cyclic loading, *J. Eng. Mat. Techn.*, Trans. ASME, **105**, pp. 113–119.
- (18) GOUGH, H. J., POLLARD, H. V. (1935) The strength of metals under combined alternating stresses, *Proc. Inst. Mechanical Engineers*, **131**, pp. 3–103.
- (19) GOUGH, H. J., POLLARD, H. V. and CLENSHAW, W. J. (1951) Some experiments on the resistance of metals to fatigue under combined stress, *Aeronautical Research Council, Reports and Memoranda*, **2522**, pp. 1–141.
- (20) PARIS, P. and ERDOGAN, F. (1963) A critical analysis of crack propagation laws, *Journal of Basic Engineering*, Trans. ASME, pp. 528–534.
- (21) DONAHUE, R. J., CLARK, H., ATANMO, P., KUMBLE, R. and McEVILY, A. J. (1972) Crack opening displacement and the rate of fatigue-crack growth, *Int. J. Fracture Mechanics*, **2**, pp. 209–219.
- (22) KLESNIL, M. and LUKAS, P. (1971) Influence of strength and stress history on growth and stabilization of fatigue cracks, CSAV Brno.
- (23) COOKE, R. J. and BEEVERS, C. J. (1973) The effect of load ratio on the threshold stresses for fatigue crack growth in medium carbon steels, *Engng Fract. Mech.*, **5**, pp. 1061–1071.
- (24) PRIDDLE, E. K. (1972) Some equations describing the constant amplitude fatigue crack propagation characteristics of a mild steel, Berkeley Nuclear Laboratories, RD/B/N 2390.
- (25) YAREMA, S. Y. (1977) Investigation of fatigue crack growth and kinetic diagrams of fatigue strength (in Russian), *Physico – Chemical Mechanics of Materials*, **8**, pp. 3–22.
- (26) RAMULU, M., KOBAYASHI, A. S. (1994) Numerical and experimental study of mixed mode fatigue crack propagation, in: *Handbook of Fatigue Crack Propagation in Metallic Structures*, (A. Carpinteri (ed), pp. 1073–1123.